APPLIED AND ENVIRONMENTAL MICROBIOLOGY, Sept. 2009, p. 5555–5562 Vol. 75, No. 17
0099-2240/09/$08.00+0 doi:10.1128/AEM.00407-09

Monochloramine Disinfection Kinetics of *Nitrosomonas europaea* by Propidium Monoazide Quantitative PCR and Live/Dead BacLight Methods[▽]

David G. Wahman, Karen A. Wulfeck-Kleier, and Jonathan G. Pressman*

United States Environmental Protection Agency, Office of Research and Development, Cincinnati, Ohio

Received 18 February 2009/Accepted 21 June 2009

Monochloramine disinfection kinetics were determined for the pure-culture ammonia-oxidizing bacterium *Nitrosomonas europaea* (ATCC 19718) by two culture-independent methods, namely, Live/Dead BacLight (LD) and propidium monoazide quantitative PCR (PMA-qPCR). Both methods were first verified with mixtures of heat-killed (nonviable) and non-heat-killed (viable) cells before a series of batch disinfection experiments with stationary-phase cultures (batch grown for 7 days) at pH 8.0, 25°C, and 5, 10, and 20 mg Cl_2/liter monochloramine. Two data sets were generated based on the viability method used, either (i) LD or (ii) PMA-qPCR. These two data sets were used to estimate kinetic parameters for the delayed Chick-Watson disinfection model through a Bayesian analysis implemented in WinBUGS. This analysis provided parameter estimates of 490 mg Cl_2-min/liter for the lag coefficient (b) and 1.6×10^{-3} to 4.0×10^{-3} liter/mg Cl_2-min for the Chick-Watson disinfection rate constant (k). While estimates of b were similar for both data sets, the LD data set resulted in a greater k estimate than that obtained with the PMA-qPCR data set, implying that the PMA-qPCR viability measure was more conservative than LD. For *N. europaea*, the lag phase was not previously reported for culture-independent methods and may have implications for nitrification in drinking water distribution systems. This is the first published application of a PMA-qPCR method for disinfection kinetic model parameter estimation as well as its application to *N. europaea* or monochloramine. Ultimately, this PMA-qPCR method will allow evaluation of monochloramine disinfection kinetics for mixed-culture bacteria in drinking water distribution systems.

As a result of stage 1 and stage 2 disinfectant and disinfection by-product rules, chloramination for secondary disinfection in the United States is predicted to increase to 57% of all surface and 7% of all groundwater treatment systems (49). A recent survey reported that 30% of the respondents currently chloraminate to maintain distribution system residual, and other recent surveys suggest that between 8 and 12% of drinking water utilities are contemplating a future switch to chloramination (3, 43).

Although chloramines are considered weaker disinfectants than chlorine for suspended bacteria, chloramines are perceived as more effective disinfectants for a biofilm (25, 53). As a result of their lower reactivity, chloramines are believed to penetrate a biofilm further and thereby to more effectively disinfect biofilm bacteria with depth than chlorine (53).

Chloramination comes with the risk of distribution system nitrification (2, 21, 22). Based on utility surveys, 30 to 63% of utilities practicing chloramination for secondary disinfection experience nitrification episodes (3, 21, 43, 54). Nitrification in drinking water distribution systems is undesirable and may result in water quality degradation (e.g., disinfectant depletion, coliform occurrences, or nitrite/nitrate formation) and subsequent noncompliance with existing regulations (e.g., surface water treatment rule or total coliform rule) (2). Thus, nitrification control is a major issue in practice and is likely to become increasingly important as chloramination increases.

Unfortunately, our understanding of distribution system nitrification and its control is incomplete, which has made this a topic of considerable ongoing research. Recently, Fleming et al. (12) proposed nitrification potential curves as a possible strategy to prevent nitrification in chloraminated drinking water distribution systems. Use of this concept or other modeling approaches inherently requires knowledge of both the growth and disinfection kinetic parameters of nitrifiers, specifically ammonia-oxidizing bacteria (AOB), inhabiting the distribution system.

Several chloramine disinfection studies have been reported for nitrifier cultures (2). However, only one study contains a detailed determination of chloramine disinfection kinetics, having investigated the pure-culture AOB *Nitrosomonas europaea* (33). In contrast to this pure-culture study, AOB are present as mixed cultures in chloraminated drinking water distribution systems, with *Nitrosomonas oligotropha* rather than *N. europaea* representing the dominant AOB found (33, 37, 38). Therefore, determination of disinfection kinetics of mixed-culture AOB likely present in chloraminated drinking water (i.e., *N. oligotropha*) represents a significant knowledge gap in our understanding of nitrification episodes.

Disinfection kinetic parameter determination inherently depends on the method used to quantify viable bacteria. In general, there are two classes of viability determinations, i.e., (i) culture-dependent and (ii) culture-independent methods (5, 16, 27). Culture-dependent methods rely on bacterial growth and include plate counts and most-probable-number (MPN)

* Corresponding author. Mailing address: United States Environmental Protection Agency, 26 W. Martin Luther King Dr., Cincinnati, OH 45268. Phone: (513) 569-7625. Fax: (513) 487-2543. E-mail: pressman.jonathan@epa.gov.

▽ Published ahead of print on 26 June 2009.

techniques. Culture-independent methods include activity measures (e.g., substrate uptake or oxygen utilization) and other methods that rely on cell membrane integrity as a viability measure. In general, culture-dependent methods result in faster disinfection kinetics than culture-independent methods.

As a first step toward gaining more information on AOB disinfection in chloraminated drinking water distribution systems, a culture-independent method with future applicability to mixed-culture AOB was implemented. In the current research, *N. europaea* was used. Even though *N. europaea* has not been found to be the dominant AOB in chloraminated systems, its use in the current research provides a comparison to existing literature. The culture-independent method combines the use of propidium monoazide (PMA), which selectively removes DNA from membrane-compromised cells and/or inhibits its amplification by PCR (29–31), with a quantitative PCR (qPCR) method developed for detection of AOB in chloraminated drinking water distribution systems (36). The results using PMA-qPCR were compared with those obtained using another culture-independent membrane integrity-based technique, the Live/Dead BacLight (LD) method. Furthermore, the experimental conditions were selected (pH 8.0 and a chlorine-to-nitrogen mass ratio of 4:1) such that monochloramine was the dominant chloramine species present, and the results are reported as monochloramine disinfection kinetics. The magnitude of the reported disinfection kinetics was closely related to the respective method used for viability determination. For example, in this research a cell was considered viable or nonviable based on the ability of propidium iodide (PI) or PMA to penetrate its membrane and on subsequent processing according to the respective method.

LD was previously used to determine detailed *N. europaea* disinfection kinetics (33) and provides a baseline comparison for the current research. Oldenburg et al. (33) provided a comparison of estimated disinfection kinetic parameters, using both the culture-dependent AOB MPN technique and LD as viability measures. The estimated disinfection kinetic parameters based on the AOB MPN method were 3 orders of magnitude greater than those obtained with the culture-independent LD method, and the lower disinfection kinetics based on LD were more consistent with AOB persistence in chloraminated drinking water distribution systems. Based on this previous research and because the AOB MPN method requires an incubation period of 21 to 30 days, it was not evaluated in the current research (2).

Initially, control experiments were conducted with various proportions of heat-killed cells to verify that both the PMA-qPCR and LD methods detected only viable cells. After the control experiments, a series of batch disinfection experiments were conducted where both PMA-qPCR and LD were utilized to quantify viable bacteria, providing two data sets for disinfection kinetic parameter estimation. Ultimately, the PMA-qPCR method used in this research will be applied to mixed-culture AOB typically present in drinking water distribution systems (i.e., *N. oligotropha*) (36–38).

MATERIALS AND METHODS

Bacterial strain and culture conditions. *N. europaea* (ATCC 19718; American Type Culture Collection, Manassas, VA) was batch grown (25 to 28°C) on a rotary shaker (100 rpm) to stationary phase (7 days) in 2.8-liter glass flasks (protected from light) with 2 liters of an inorganic salt medium (23). The inorganic salt medium consisted of 5.0 mM $(NH_4)_2SO_4$ (140 mg N/liter total ammonia), 0.40 mM KH_2PO_4, 1.0 mM KCl, 0.20 mM $MgSO_4 \cdot 7H_2O$, 1.0 mM $CaCl_2 \cdot 2H_2O$, and 10 mM NaCl, with the addition of 0.2 ml phenol red (0.5%) and 1 ml trace element stock solution per liter of medium. The trace element stock solution consisted of 0.02 mM $MnCl_2 \cdot 4H_2O$, 0.80 mM H_3BO_3, 0.15 mM $ZnSO_4 \cdot 7H_2O$, 0.030 mM $(NH_4)_6Mo_7O_{24} \cdot 4H_2O$, 3.5 mM $FeSO_4 \cdot 7H_2O$, 0.10 mM $CuCl_2 \cdot 2H_2O$, and 0.025 mM 6 N HCl. To maintain pH, 0.2-μm-pore-size filter-sterilized 5% (wt/vol) $NaHCO_3$ was added based on the color change of the phenol red indicator from red to yellow, indicating a drop in medium pH. Culture purity was checked by confirming cell morphology via microscopy with an Axioplan 2/Axiophot 2 microscope (Carl Zeiss Micro Imaging, Inc., Thornwood, NY), and the presence of heterotrophic contamination was checked by plating on R2A agar.

Monochloramine preparation and measurement. Free chlorine solutions were prepared by diluting 4 to 6% NaOCl with ultrapure water (Barnstead NANOpure Diamond; Barnstead International, Dubuque, IA) as required. Stock NaOCl solutions were standardized periodically with sodium thiosulfate in accordance with standard method 4500B (1). Ammonium sulfate $[(NH_4)_2SO_4]$ was dissolved in ultrapure water, with the addition of chlorine solutions at a 4:1 chlorine-to-nitrogen (Cl_2:N) mass ratio to form monochloramine. Monochloramine was measured on a Nicolet Evolution 300 UV-visible spectrophotometer (Thermo Electron Scientific Instruments, Madison, WI) at 655 nm, using Hach method 10171, allowing detection of only monochloramine (26). Total and free chlorine measurements were measured on a DR/2500 spectrophotometer (Hach Company, Loveland, CO) at 530 nm, using Hach methods 8167 and 8021, respectively. Under our experimental conditions (pH 8.0, 25°C, 4:1 Cl_2:N mass ratio, 10 mM phosphate concentration, and 5, 10, and 20 mg Cl_2/liter total chlorine), monochloramine was the dominant species. This was confirmed by experimental measurements and further supported by implementation of a monochloramine autodecomposition model (20, 51) in the computer program AQUASIM (EAWAG, Dübendorf, Switzerland) (39). Under the modeled experimental conditions, monochloramine comprised >99% of the total chlorine present.

LD. LD kit L7012 (Invitrogen, Carlsbad, CA) for microscopy and quantitative assays was used according to the manufacturer's instructions to differentiate viable and nonviable *N. europaea* cells. A 20-μl sample (based on approximately 1×10^8 cells/ml) was diluted in 10 ml sterile phosphate-buffered saline (PBS; 10 mM Na_2HPO_4 and 130 mM NaCl, pH 8) and vortexed briefly. This sample was then filtered through a 0.2-μm black polycarbonate filter under vacuum to create the prepared sample.

With protection of components from light, 3 μl component A (Syto 9) and 3 μl component B (PI) were added to 2 ml sterile PBS. This solution was then added to the prepared sample for direct staining on the filter and incubated for 15 min in the dark. After staining of the sample, the residual stain was removed by applying a vacuum to the prepared sample. The filter was then placed on a precleaned microscope slide, and 2 drops of component C (BacLight mounting oil) was placed on the filter surface before it was covered with a coverslip. The cells were visualized using a microscope equipped with an AxioCam MRm digital camera, AxioVision 3.1 image analysis software, and filter sets 9 and 15 (Carl Zeiss Micro Imaging, Inc., Thornwood, NY) to capture the green (viable) and red (nonviable) fluorescing cells. With a magnification of ×400, at least 10 fields were randomly chosen for each sample. Two images were taken for each field (one for each filter set) and later combined into a single image for manual counting, resulting in determinations of the number of viable cells (N), number of total cells (N_T), and ratio of viable to total cells (N/N_T).

PMA treatment. PMA treatment was conducted according to the method of Nocker et al. (31). Briefly, PMA (Biotium, Inc., Hayward, CA) was dissolved in 20% dimethyl sulfoxide, creating a 20 mM PMA stock solution. This stock solution was stored at −20°C in the dark. PMA was added to culture aliquots (1.75 ml) to a final PMA concentration of 50 μM in 2-ml microcentrifuge tubes and vortexed briefly. These samples were then incubated in the dark for 5 min before being exposed to light for 2 min at a distance of 20 cm from a 650-W halogen light source (Sachtler R651HS; Camera Dynamics, Inc., Valley Cottage, NY). To avoid excessive heating, the samples were laid horizontally on ice and rotated every 30 s. After PMA treatment, the cells were harvested by centrifugation at 5,000 × g for 10 min prior to DNA isolation.

DNA isolation and quantification. Genomic DNA was extracted using a DNeasy blood and tissue kit (Qiagen, Valencia, CA) according to the manufacturer's instructions for gram-negative bacteria. Extracted DNA was visualized in 1% agarose gels stained with Lonza GelStar nucleic acid gel stain (Cambrex, East Rutherford, NJ) to assess their integrity. For each sample, triplicate DNA extractions were performed to account for variations in extraction efficiency.

TABLE 1. qPCR primer and probe summary for *amoA* gene target[a]

Primer or probe	Name	Sequence (5′–3′)
Forward primer	amoA-1F	GGG GTT TCT ACT GGT GGT
Reverse primer	amoA-2R	CCC CTC KGS AAA GCC TTC TTC
TaqMan probe	amoA-Nm3	TGT CGA TGG CTG AYT ACA TGG G

[a] From reference 36.

Quantitative real-time PCR. The method of Regan et al. (36) was used to perform qPCR, using *amoA* gene target primers and probe (Table 1). Each 25-μl qPCR mix contained 12.5 μl 2× TaqMan gene expression master mix (Applied Biosystems, Foster City, CA), 1 μl each of forward and reverse primers (Sigma-Genosys, The Woodlands, TX) at a 200 nM final concentration, 0.5 μl of 6-carboxyfluorescein-labeled TaqMan probe (Sigma-Genosys, The Woodlands, TX) at a 100 nM final concentration, 2.5 μl bovine serum albumin (Fisher Scientific, Pittsburgh, PA) at a 0.1-mg/ml final concentration, 2.5 μl water, and 5 μl DNA template. For analysis, qPCR was performed on a 7900HT fast real-time PCR system (Applied Biosystems, Foster City, CA), using the following thermal profile: (i) an initial 10-min step at 95°C; (ii) 40 cycles of (a) 40 s at 95°C, (b) 60 s at 58°C, and (c) 45 s at 72°C; and (iii) a final 60-s extension step at 72°C. All reactions were performed in triplicate in MicroAmp fast optical 96-well reaction plates with optical adhesive film (Applied Biosystems, Foster City, CA). Data were analyzed with Sequence Detection Systems software, version 2.3.2 (Applied Biosystems, Foster City, CA). Cycle threshold numbers and baselines were automatically determined by the software. The sizes of PCR products were verified with a 2% agarose gel stained with Lonza GelStar nucleic acid gel stain, utilizing an AlphaQuant 6 molecular ladder (Alpha Innotech, San Leandro, CA).

For each qPCR plate analyzed, a standard curve was generated using triplicate 10-fold serial dilutions of plasmid DNA containing the target gene (*amoA*) as an insert, generating samples ranging from approximately 10^2 to 10^8 copies of target DNA per reaction. Plasmid concentrations were quantified with a NanoDrop ND-1000 UV spectrophotometer (Thermo Fisher Scientific, Wilmington, DE). The plasmid copy number per standard sample was derived from equation 1 as follows:

$$C_{amoA} = \frac{N_A V_R C_P}{P_{BP} \mathrm{MW}_{BP}} \quad (1)$$

where C_{amoA} is the number of *amoA* copies per reaction, N_A is the Avogadro constant (6.022×10^{23} copies/mole), V_R is the amount of plasmid DNA added to each PCR mix (5 μl/reaction), C_P is the plasmid DNA concentration quantified by UV spectrophotometry (g/μl), P_{BP} is the size of the plasmid DNA (vector plus PCR amplicon) (bp), and MW_{BP} is the average DNA molecular weight (660 g/mol/bp).

Figure 1 details a typical standard curve generated by plotting the calculated *amoA* gene copy number per reaction versus the cycle threshold number. A minimum of three nontemplate controls were performed for each qPCR plate. PMA-qPCR analysis resulted in an estimate of the number of viable cells (N) in a given sample, using the fact that the *N. europaea* genome contains two copies of the *amoA* gene (6).

Heat-killed cell control experiments. *N. europaea* was harvested from batch growth by centrifugation (4,500 × *g* for 20 min) 7 days after inoculation, washed, centrifuged again, and resuspended in an equal volume of fresh 0.2-μm filter-sterilized PBS. Culture aliquots (approximately 1×10^8 cells/ml) of 3 ml were transferred to 6-ml polypropylene round-bottomed tubes with caps (BD Falcon, Franklin Lakes, NJ) and heat killed for 15 min at 72°C in a laboratory heat block. The samples were vortexed after every 5 minutes of incubation. After 15 min, these samples were immediately placed on ice. Various defined ratios of heat-killed (nonviable) and non-heat-killed (viable) cells were combined and processed by either LD or PMA-qPCR.

Batch disinfection experiments. For each duplicate experiment, 800 ml *N. europaea* was harvested from batch growth by centrifugation (4,500 × *g* for 20 min) 7 days after inoculation, washed, centrifuged again, and resuspended in 20 ml fresh 0.2-μm filter-sterilized PBS. Washed cells were maintained in PBS for 24 h at 25°C on a rotating shaker (100 rpm) before experiments to allow recovery from any centrifugation-induced cell damage (33). All experiments were conducted at pH 8.0 and 25°C. Glassware was made chlorine demand-free by soaking in a 5,000-mg Cl_2/liter concentrated free chlorine solution for 24 h, rinsed with distilled water, and air dried.

For each experiment, 400 ml filter-sterilized (0.2-μm pore size) PBS received approximately 10 ml harvested cells (approximate final cell concentration of 1×10^8 cells/ml). While the cultures were mixed vigorously on a magnetic stir plate, two samples were taken for initial and final monochloramine-free controls. The remainder of the solution was spiked with the desired monochloramine concentration. The PBS-cell suspension was aliquoted in headspace-free vials and placed in a dark incubation shaker (100 rpm). Samples were sacrificed over time and analyzed for pH, monochloramine, total ammonia, total cell counts, and viability by LD and PMA-qPCR. At least duplicate experiments were conducted for each monochloramine concentration tested (5, 10, and 20 mg Cl_2/liter monochloramine).

The LD method used a filtering step to remove the disinfectant. The disinfection time was recorded at the conclusion of filtration because the bacteria remained exposed to disinfectant. For PMA-qPCR, the samples were dechlorinated by adding sodium sulfite (Na_2SO_3) from a 2,300-mg/liter stock solution prepared the day of the experiment and then vortexed briefly. Na_2SO_3 dosing was based on a ratio of 2.3 mg Na_2SO_3 per mg NH_2Cl as Cl_2 (theoretical stoichiometric ratio plus 0.50 mg Na_2SO_3 per mg NH_2Cl as Cl_2) (48). For PMA-qPCR samples, the disinfection time was recorded at the time of Na_2SO_3 addition. Monochloramine quenching was verified in each experiment with a Na_2SO_3-dosed control sample. Bacterial dispersion was verified by direct microscopic observation of single cells with no clustering. In all modeling efforts, the average monochloramine concentration was used because monochloramine decreased, on average, less than 5% from the initial to the final measurements (data not shown).

For each batch disinfection experiment, a series of controls was included. For LD, a heat-killed control sample was prepared and analyzed as previously described. For PMA-qPCR, the following controls were included: (i) heat-killed sample (a) with and (b) without PMA treatment, (ii) PBS (a) with and (b) without PMA treatment, (iii) heat-killed sample with PMA treatment and Na_2SO_3 addition, (iv) initial samples with PMA treatment and (a) with and (b) without Na_2SO_3 addition, and (v) final samples with PMA treatment and (a) with and (b) without Na_2SO_3 addition.

Estimation of disinfection kinetic parameters and credible regions. The delayed Chick-Watson model was used for parameter estimation (equation 2) (10), as follows:

$$\ln \frac{N/N_T}{N_0/N_T} = \ln \frac{N}{N_0} = \begin{cases} 0 & \text{for } Ct \le b \\ -k(Ct - b) & \text{for } Ct > b \end{cases}$$
$$\ln N = \begin{cases} \ln N_0 & \text{for } Ct \le b \\ \ln N_0 - k(Ct - b) & \text{for } Ct > b \end{cases} \quad (2)$$

where C is the disinfectant concentration (mg Cl_2/liter), t is time (min), k is the disinfectant rate constant (liters/mg Cl_2-min), b is the lag coefficient (mg Cl_2-min/liter), N is the number of viable bacteria at t, N_0 is the initial number of viable bacteria at $t = 0$, N_T is the total number of bacteria at t, N/N_T is the viable bacteria ratio at t, and N_0/N_T is the initial viable bacteria ratio at $t = 0$. Equation 2 accounts for an initial lag phase where no disinfection occurs followed by a pseudo-first-order phase, representing traditional Chick-Watson disinfection kinetics (i.e., the delayed Chick-Watson model reduces to the Chick-Watson model if the lag coefficient [b] equals zero).

The form of equation 2 accounts for the two viability measurements used in this research, where estimates of N/N_T and N were provided by LD and PMA-qPCR, respectively. The lag coefficient (b), disinfectant rate constant (k), and

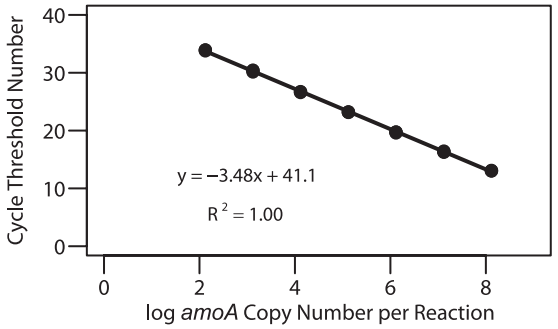

FIG. 1. Example qPCR standard curve for *N. europaea*, using *amoA* gene target plasmid DNA.

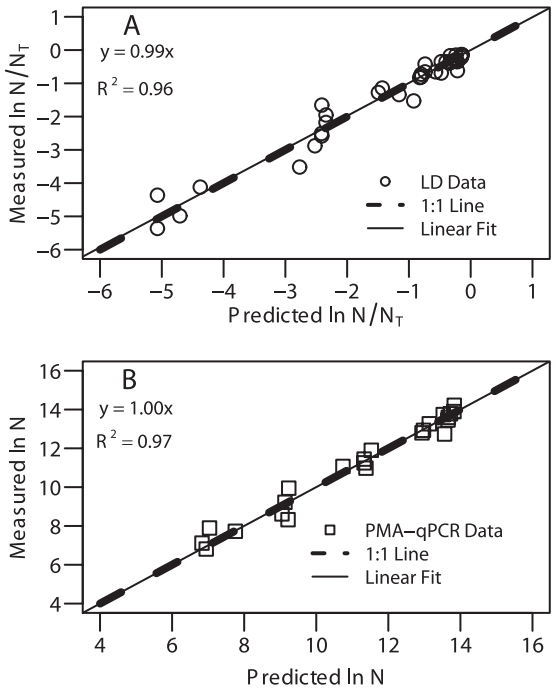

FIG. 2. Heat-killed cell control experimental data for LD (A) and PMA-qPCR (B) methods.

initial number of viable bacteria (N_0) for the delayed Chick-Watson model were determined by Bayesian statistical methods following the method of Sivaganesan et al. (46), with N_0 as an additional parameter to account for the inaccuracy of the time zero viable cell measurement. The random error was assumed to be normally distributed, with a mean of 0 and a variance of σ^2. The priors used in the current research are similar to those used in previous Bayesian analyses involving the delayed Chick-Watson model (45, 46). The purpose of the priors is to incorporate prior information about the unknown parameters. Because no prior information is assumed for the unknown parameters k and N_0, a diffuse (i.e., noninformative) normal prior was used, with a mean of 0 and a variance of 10^6. Similarly, for σ^2, a diffuse inverse-gamma (0.001, 0.001) prior was used, which approximates Jeffrey's prior $\text{pr}(\sigma^2) \propto 1/\sigma^2$. As done in previous research (45, 46) and because it is reasonable to assume that b could occur anywhere in the range of the experimental Ct data, a uniform prior distribution for b was assumed, between 0 and the maximum Ct value (Ct_{max}) during the experiments. These priors are written as follows: $k \sim N(0, 10^6)$, $N_0 \sim N(0, 10^6)$, $\sigma^2 \sim$ inverse-gamma (0.001, 0.001), and $b \sim$ uniform (0, Ct_{max}).

According to Bayes's rule, the posterior distribution of the model parameters (k, N_0, b, and σ^2) given by the data is proportional to the product of the prior distribution and likelihood. The Markov chain Monte Carlo method was implemented through WinBUGS software (28; http://www.mrc-bsu.cam.ac.uk/bugs/). WinBUGS was used for estimation of parameters and generation of 95% credible intervals.

The 95% bivariate highest-posterior-density (HPD) region was determined using the posterior distributions of k and b to provide a clearer picture of the parameter estimates. Sampling from the posterior distribution generated from WinBUGS was imported into the statistical computing and graphics software R (35; http://www.r-project.org/). In R, HPDregionplot from the emdbook package (4) was used for generation of the HPD contour. From the imported Markov chain Monte Carlo-generated posterior distributions, HPDregionplot used kde2d from the MASS package (50) to calculate a two-dimensional kernel density on a square grid, normalized the plot, and calculated the contour corresponding to a two-dimensional HPD region for the specified (i.e., 95%) probability level.

Analytical methods. Bacterial cell concentrations were determined by direct cell enumeration, using a Helber Bacteria Z30000 (Hawksley, Lancing, Sussex, United Kingdom) cell counting chamber. pH and total ammonia were measured on a model 250 pH-ISE-conductivity meter with a pH electrode and ammonia-ion-selective electrode (Denver Instrument, Denver, CO), respectively.

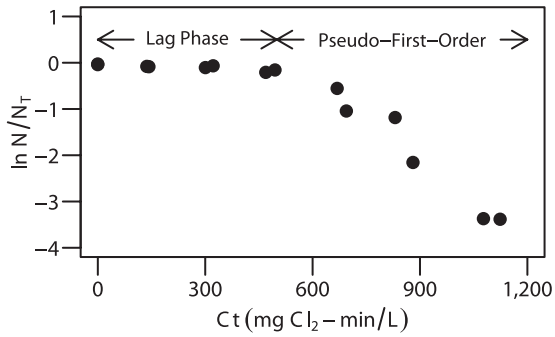

FIG. 3. Example of disinfection trend seen during batch disinfection experiments (experimental data shown for 5 mg Cl_2/liter monochloramine with LD).

RESULTS AND DISCUSSION

Control experiments. Heat-killed cell control experiments were conducted by mixing various known proportions of heat-killed (nonviable) and non-heat-killed (viable) *N. europaea* cells. These mixtures were then quantified using both LD and PMA-qPCR to verify the ability of each method to selectively measure only viable cells. Figure 2 summarizes the results from these experiments, showing the measured versus predicted (based on the known proportions) natural logarithms of viable cell ratios (N/N_T) for LD and viable cells (N) for PMA-qPCR, the theoretical 1:1 line, and the best-fit line based on the experimental data. These results verify that both methods are able to selectively measure viable cells in a mixture of viable and nonviable cells for *N. europaea*. Although PMA treatment has been shown to selectively remove and/or inhibit PCR amplification of DNA from various heat-killed bacteria (30, 31), this is the first demonstration of its application to *N. europaea*.

Batch disinfection experiments. Figure 3 shows a representative example of the *N. europaea* disinfection trend observed during batch disinfection experiments. An initial lag phase was observed, characterized by little or no disinfection, followed by pseudo-first-order disinfection kinetics. Previous research attributed the presence of a lag phase to disinfection resistance caused by bacterial aggregation (52), but in the current research, direct microscopic observations performed during the experiments showed only single cells with no discernible aggregation, eliminating bacterial aggregation as a possible explanation for the lag phase.

The presence of a lag phase during monochloramine disinfection is not surprising based on its proposed disinfection mechanism from studies involving *Escherichia coli* B (17–19). In these studies, monochloramine reacted rapidly with only four amino acids (cysteine, cystine, methionine, and tryptophan) and very slowly with DNA and RNA and did not severely damage the cell envelope of *E. coli* B. In all, this previous research supports the multiple-hit monochloramine disinfection concept whereby monochloramine reacts at several sensitive sites in bacteria before the bacteria become inactivated (18). The multiple-hit concept may explain the lag phase because the multiple reactions leading to disinfection proceed slowly.

Disinfection model selection. The prevalence of a lag (shoulder) phase in the experimental data resulted in selection of a

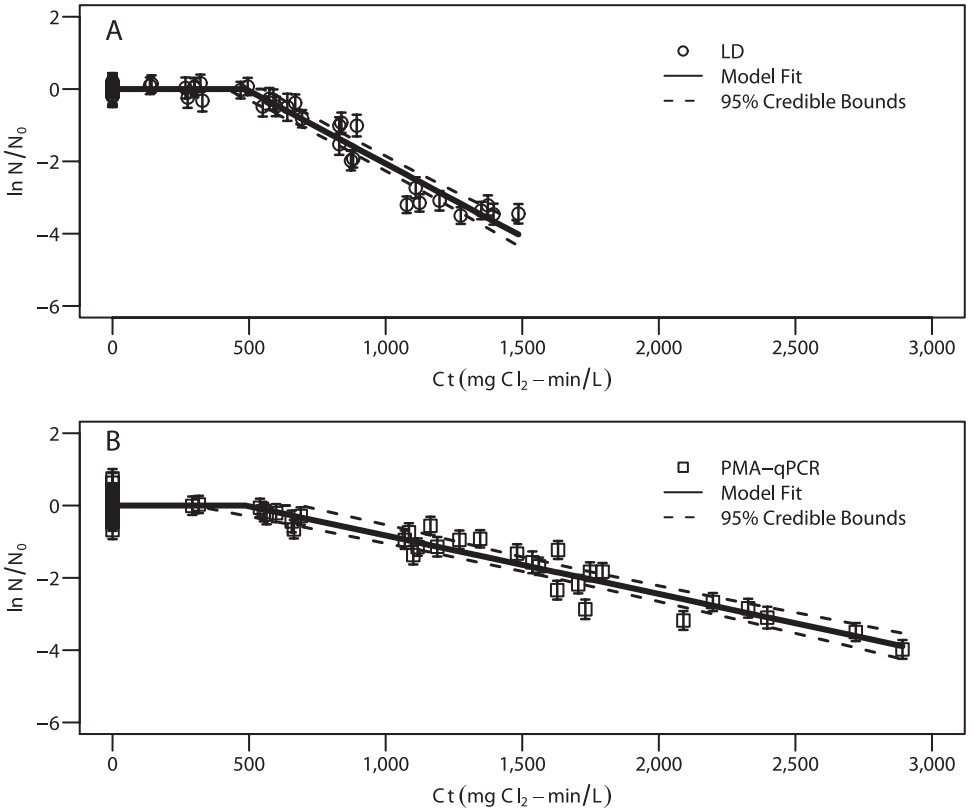

FIG. 4. Delayed Chick-Watson model fits and 95% credible bounds for LD (A) and PMA-qPCR (B) experimental data (data shown for all experimental conditions).

disinfection kinetic model that could account for it (delayed Chick-Watson model). The selection of the delayed Chick-Watson model was based on an evaluation that incorporated both the observed experimental data and practical concerns for the intent of the research undertaken. There is a substantial literature base establishing the delayed Chick-Watson model as an appropriate model for disinfection data with an apparent lag phase (e.g., see references 8, 11, 24, 40–42, and 47). Other disinfection models account for lag (e.g., the Hom-Hass model [13–15] and the series-event model [44]), but selection of the delayed Chick-Watson model allowed the initial lag phase to be accounted for with a lag coefficient (*b*) that is consistent with the concentration-time (*Ct*) concept of disinfection, providing a physical meaning for *b* (i.e., the *Ct* required to overcome the initial lag phase during disinfection). In addition, the *Ct* concept is used by the USEPA to regulate water disinfection (10); therefore, in this research, it was desired to use a model consistent with the *Ct* concept.

Previous research on monochloramine disinfection kinetics with *N. europaea* used the Chick-Watson model (33), and all published monochloramine disinfection research with ammonia-oxidizing bacteria (2, 7) has utilized the Chick-Watson model for determination of disinfection kinetics. It was determined that to maintain a direct comparison to these data, the delayed Chick-Watson model represented an appropriate model choice to incorporate the lag phase, as the rate constants are directly comparable. Furthermore, based on the results of this research (Fig. 4; see following discussion), the delayed Chick-Watson model was representative of the experimental data and was a reasonable choice to model the disinfection kinetics. Therefore, a combination of the good agreement between the delayed Chick-Watson model and the experimental data and the practical considerations for maintaining the *Ct* concept led to the use of the delayed Chick-Watson model to incorporate the apparent lag phase.

Estimation of disinfection kinetic parameters and credible regions. The delayed Chick-Watson model was implemented in WinBUGS software and used to estimate the model parameters and their 95% credible bounds for each data set (LD and PMA-qPCR). In the WinBUGS analysis, six chains were simulated at various initial values for parameters. An initial simulation of 30,000 iterations was performed as a burn-in before a further 6,000 iterations were used to estimate the model parameter posterior distributions. The convergence diagnostics present in WinBUGS (trace plots, autocorrelation plots, and Gelman and Rubin diagnostics) found the convergence to be satisfactory (data not shown) (9). Experimental results and the resulting model fit and 95% credible bounds are shown in Fig. 4 for the LD and PMA-qPCR data sets. The ordinates in Fig. 4 display the natural logarithms of experimental data points (N) divided by the estimated model parameter (N_0). Because N represents experimental data and N_0 is estimated, the error bars in Fig. 4 correspond to the uncertainty in the N_0 estimate. Figure 4 details the ability of the delayed Chick-Watson model to provide an adequate explanation for the experimental data for both the LD and PMA-qPCR data sets,

TABLE 2. Disinfection kinetic parameter (b and k) summary and calculated Ct_{99} values

Data set	b (mg-min/liter) (mean ± SD)	k (10^{-3} liter/mg-min) (mean ± SD)	Ct_{99} (mg-min/liter)
LD	490 ± 35	4.0 ± 0.23	1,600
PMA-qPCR	490 ± 100	1.6 ± 0.12	3,300
Oldenburg et al. (33)[a]	ND	2.0	2,300

[a] Adjusted to 25°C by using an activation energy for monochloramine of 77 kJ/mol (10). ND, not determined.

where an initial lag period is followed by pseudo-first-order disinfection. It is evident from Fig. 4 that both viability measures provided similar estimates of the lag coefficient, as shown by the similar Ct values for the lag phase (horizontal line), but the estimated disinfection rate constants differed, as shown by the different slopes of the postlag inactivation curves.

Because LD and PMA-qPCR experiments were conducted simultaneously, the only experimental difference was the viability method. The different LD and PMA-qPCR kinetics can be explained by at least two possibilities related to the extent of cell membrane damage required to elicit a response from each respective method. The first possibility is simply that the two different chemicals, PI and PMA, which have slightly different chemical sizes, require a different degree of cell membrane damage to enter a cell based on the principal of size exclusion. Because PMA is larger than PI, it follows that PMA might require more cell membrane damage to enter and may thus result in slower disinfection kinetics. A second possibility results from the differences in processing of each method, whereby the different disinfection kinetics are caused by the differences between fluorescence staining and visualization (PI) versus DNA intercalation and physical removal via centrifugation and/or suppression of amplification during qPCR (PMA). Because each chemical is used in a different process, differences in process efficiency can lead to the differences in reported results. In all, the current results suggest that the PMA-qPCR method requires a greater degree of cell membrane damage than LD before the method elicits a nonviable response.

Table 2 summarizes the results from the data analysis for the estimated kinetic parameters (b and k) and calculated Ct_{99} values (Ct required for 99% disinfection) based on the estimated model parameters. For comparison purposes, the temperature-adjusted value (from 20°C to 25°C, using an activation energy of 77 kJ/mol [10]) from the work of Oldenburg et al. (33) at pH 8.0 is included in Table 2. LD and PMA-qPCR produced identical estimates for b, but the LD estimate for k is 2.5 times as great as that for PMA-qPCR. This results in the PMA-qPCR Ct_{99} being approximately twice as great as the LD Ct_{99}. Compared to previous research, the LD k is twice as great as that determined by Oldenburg et al. (33), but the LD Ct_{99} is only 0.7 times as great because of the lag phase. Overall, Ct_{99} values for all three analyses were within a factor of 2, with the order PMA-qPCR value > value of Oldenburg et al. (33) > LD value.

To provide a clearer picture of the uncertainty in the estimated model parameters (b and k), Fig. 5 displays the joint 95% HPD regions, detailing the positive correlation between b and k for LD and PMA-qPCR. In Fig. 5, samples from the posterior distributions are shown with their generated 95% HPD contour. The areas in Fig. 5 highlight the greater uncertainty in the estimate of b with PMA-qPCR and the difference in k between the two methods. Even though both methods produced identical estimates of b, it is clear from Fig. 5, because of the different areas encompassed by the LD and PMA-qPCR 95% HPD contours, that LD and PMA-qPCR result in significantly different estimates of the coupled disinfection kinetic parameters. Overall, viability determination with PMA-qPCR provided a more conservative measure of disinfection than that obtained with LD.

Lag phase. As mentioned previously, disinfection kinetics are inherently tied to the method used to quantify viable bacteria (i.e., LD or PMA-qPCR). Therefore, it was interesting to know whether the observed lag phase could somehow be a result of the selection of viability methods. However, while in the current research there was an observed lag phase at pH 8.0, in previous research with LD and *N. europaea* (33) there was no lag phase observed at pH 8.0. Because both of these research efforts were conducted under similar conditions, except for the bacterial growth state, it appears that the lag phase was not a specific result of the viability methods. Rather, the presence of a lag phase was more likely the result of the different growth methods employed. Stationary-phase batch-grown cultures were used in the current research, in contrast with continuous-growth chemostat cultures in previous research (33). Additionally, while Oldenburg et al. (33) did not present an analysis of their data for any presence of lag phase, their pH 9.0 data appear to show a lag phase. In a recent study, the appearance of a lag phase with increasing pH was reported for monochloramine disinfection of adenovirus serotype 2 (47). In these adenovirus serotype 2 experiments conducted at 20°C, no lag phase was present for experiments conducted at pH 6 and 8, but the disinfection curve at pH 10 was characterized by a lag phase followed by pseudo-first-order kinetics (47). Inherently, using the Chick-Watson model when a lag phase is present will lead to a lower estimation of k than that with the delayed Chick-Watson model for the same data set (data not shown).

Practical significance. The monochloramine disinfection kinetics in the current research may have implications for drinking water distribution systems using monochloramine and having the presence of a biofilm. For example, a survey of systems using monochloramine as a secondary disinfectant indicated that the median monochloramine residual at the distribution system maximum residence time was 1 mg Cl_2/liter (43). With this 1-mg Cl_2/liter monochloramine residual, it would require approximately 8 h of contact time to overcome the initial lag phase and an additional 19 to 47 h to achieve 99% disinfection of the bacteria (Ct_{99}), which is significant considering that AOB generation times are on the order of 8 to 50 h (34). For a biofilm present on the pipe wall in a distribution system, the contact times are expected to be even longer because the monochloramine concentration is expected to decrease with depth into the biofilm, resulting from reaction and diffusion of monochloramine. The reduced monochloramine concentration with biofilm depth would increase the contact time required to overcome the lag phase and subsequent disinfection.

Previous research (33) showed that disinfection kinetics obtained by LD were more consistent with AOB persistence in

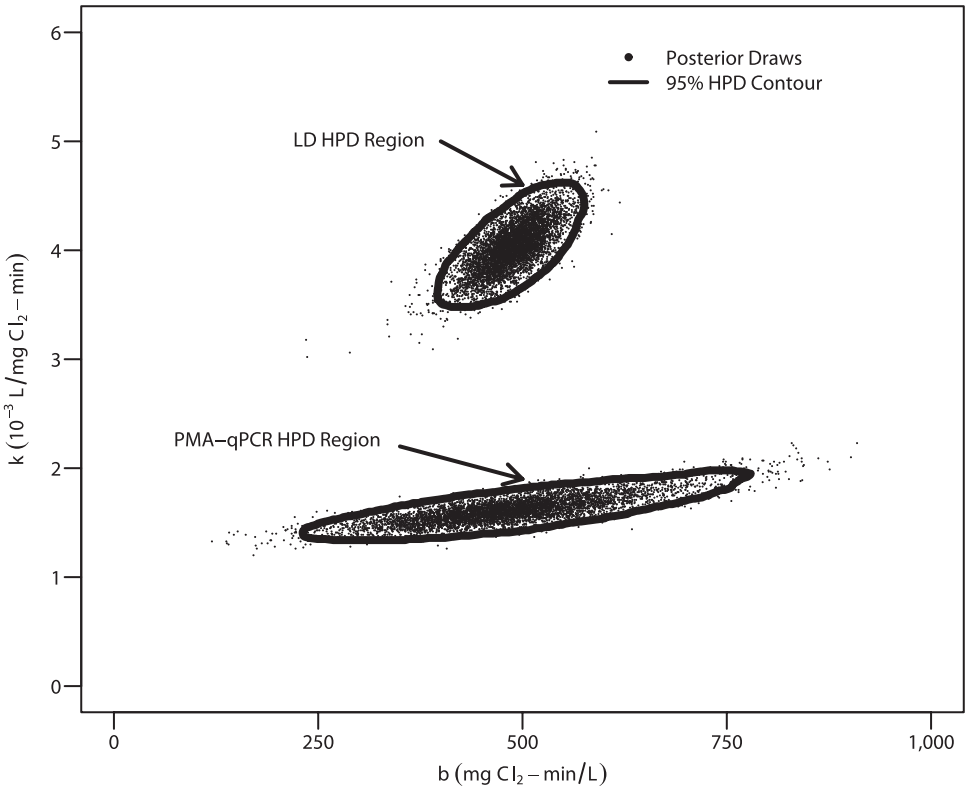

FIG. 5. Posterior distribution draws (6,000 draws from chain 1 are displayed) and associated 95% joint HPD region for the delayed Chick-Watson model kinetic parameters estimated using the LD and PMA-qPCR data.

chloraminated drinking water distribution systems than the disinfection kinetics resulting from the AOB MPN culture-dependent viability assay. Following from that study, the PMA-qPCR results are significantly closer to the LD results than the AOB MPN results from the previous research (33), and it is expected that the PMA-qPCR results will also be more consistent with AOB persistence than the AOB MPN method. At this time, it is not possible to discern which of the methods tested in this research better represent AOB disinfection in practice; however, further research will provide additional information in hopes of providing insight into how well either LD- or PMA-qPCR-based disinfection kinetics reflect systems in practice.

Summary. Overall, for the LD and PMA-qPCR data sets, the delayed Chick-Watson model parameter estimates led to similar values of *b*. However, each data set led to a significantly different value of *k*, with the PMA-qPCR data set resulting in a lower value of *k*. In general, the delayed Chick-Watson model closely simulated the monochloramine disinfection of *N. europaea*, where an initial lag phase was followed by pseudo-first-order disinfection kinetics. Viability determination by PMA-qPCR provided a more conservative measure of disinfection than that obtained by LD.

This is the first application of a PMA-qPCR method for (i) direct comparison with LD as a viability measure during disinfection, (ii) use with monochloramine as a disinfectant, (iii) use with any nitrifiers and specifically *N. europaea*, and (iv) estimation of fundamental disinfection kinetic parameters, extending the previous work of Nocker et al. (31), who showed that qPCR cycle threshold numbers increased with increasing disinfection strength but did not attempt to estimate disinfection kinetic parameters.

The PMA-qPCR method in this research will allow determination of monochloramine disinfection kinetics for mixed-culture AOB present in drinking water distribution systems. Furthermore, the methodology described herein is applicable to other disinfectants that damage the cellular membrane and are thus amenable to PMA as a measure of viability and to other organisms for which a qPCR method can be or is already developed.

ACKNOWLEDGMENTS

We thank Mano Sivaganesan and Mary Schoen for assistance with Bayesian analysis; Andrew Carroll, Brandt Miller, Charlotte Smith, and Lauren Zalla for work with Live/Dead BacLight samples; Mike Ware for microscope use; the Microbial Contaminants Control Branch for use of their qPCR equipment and lab space; and Gerald E. Speitel, Jr., and John M. Regan for plasmids.

The U.S. Environmental Protection Agency, through its Office of Research and Development, conducted the research described herein. It has been subjected to the agency's peer and administrative review and has been approved for external publication. Any opinions expressed are those of the authors and do not necessarily reflect the views of the agency, and therefore no official endorsement should be inferred. Any mention of trade names or commercial products does not constitute endorsement or recommendation for use.

REFERENCES

1. **American Public Health Association.** 1998. Standard methods for the examination of water and wastewater, 20th ed. American Public Health Association, Washington, DC.

2. **American Water Works Association.** 2006. Fundamentals and control of nitrification in chloraminated drinking water distribution systems (AWWA manual M56), 1st ed. American Water Works Association, Denver, CO.
3. **AWWA Water Quality and Technology Division Disinfection Systems Committee.** 2008. Committee report: disinfection survey, part 2—alternatives, experiences, and future plans. J. Am. Water Works Assoc. **100:**110–124.
4. **Bolker, B.** 2007, posting date. emdbook: ecological models and data (book support). R package, version 1.1.1. http://cran.r-project.org/web/packages/emdbook/index.html.
5. **Breeuwer, P., and T. Abee.** 2000. Assessment of viability of microorganisms employing fluorescence techniques. Int. J. Food Microbiol. **55:**193–200.
6. **Chain, P., J. Lamerdin, F. Larimer, W. Regala, V. Lao, M. Land, L. Hauser, A. Hooper, M. Klotz, J. Norton, L. Sayavedra-Soto, D. Arciero, N. Hommes, M. Whittaker, and D. Arp.** 2003. Complete genome sequence of the ammonia-oxidizing bacterium and obligate chemolithoautotroph *Nitrosomonas europaea*. J. Bacteriol. **185:**2759–2773.
7. **Chauret, C., C. Smith, and H. Baribeau.** 2008. Inactivation of Nitrosomonas europaea and pathogenic Escherichia coli by chlorine and monochloramine. J. Water Health **6:**315–322.
8. **Corona-Vasquez, B., J. L. Rennecker, A. M. Driedger, and B. J. Marinas.** 2002. Sequential inactivation of *Cryptosporidium parvum* oocysts with chlorine dioxide followed by free chlorine or monochloramine. Water Res. **36:**178–188.
9. **Cowles, M. K., and B. P. Carlin.** 1996. Markov chain Monte Carlo convergence diagnostics: a comparative review. J. Am. Stat. Assoc. **91:**883–904.
10. **Crittenden, J. C., R. R. Trussell, D. W. Hand, K. J. Howe, and G. Tchobanoglous (ed.).** 2005. Water treatment: principles and design, 2nd ed. John Wiley & Sons, Hoboken, NJ.
11. **Driedger, A. M., J. L. Rennecker, and B. J. Marinas.** 2001. Inactivation of *Cryptosporidium parvum* oocysts with ozone and monochloramine at low temperature. Water Res. **35:**41–48.
12. **Fleming, K. K., G. W. Harrington, and D. R. Noguera.** 2008. Using nitrification potential curves to evaluate full-scale drinking water distribution systems. J. Am. Water Works Assoc. **100:**92–103.
13. **Haas, C. N., and J. Joffe.** 1994. Disinfection under dynamic conditions: modification of Hom's model for decay. Environ. Sci. Technol. **28:**1367–1369.
14. **Haas, C. N., and S. B. Karra.** 1984. Kinetics of microbial inactivation by chlorine. I. Review of results in demand-free systems. Water Res. **18:**1443–1449.
15. **Haas, C. N., and S. B. Karra.** 1984. Kinetics of microbial inactivation by chlorine. II. Kinetics in the presence of chlorine demand. Water Res. **18:**1451–1454.
16. **Hoefel, D., W. L. Grooby, P. T. Monis, S. Andrews, and C. P. Saint.** 2003. Enumeration of water-borne bacteria using viability assays and flow cytometry: a comparison to culture-based techniques. J. Microbiol. Methods **55:**585–597.
17. **Jacangelo, J. G.** 1986. Mechanism of microbial inactivation by monochloramine. Dissertation. The John Hopkins University, Baltimore, MD.
18. **Jacangelo, J. G., V. P. Olivieri, and K. Kawata.** 1991. Investigating the mechanism of inactivation of *Escherichia coli* B by monochloramine. J. Am. Water Works Assoc. **83:**80–87.
19. **Jacangelo, J. G., V. P. Olivieri, and K. Kawata.** 1987. Oxidation of sulfhydryl groups by monochloramine. Water Res. **21:**1339–1344.
20. **Jafvert, C. T., and R. L. Valentine.** 1992. Reaction scheme for the chlorination of ammoniacal water. Environ. Sci. Technol. **26:**577.
21. **Kirmeyer, G., K. Martel, G. Thompson, L. Radder, W. Klement, M. LeChevallier, H. Baribeau, and A. Flores.** 2004. Optimizing chloramine treatment, 2nd ed. AWWA Research Foundation, Denver, CO.
22. **Kirmeyer, G. J., L. H. Odell, J. Jacangelo, A. Wilczak, and R. Wolfe.** 1995. Nitrification occurrence and control in chloraminated water systems. AWWA Research Foundation, Denver, CO.
23. **Koops, H. P., B. Bottcher, U. C. Moller, A. Pommerening-Roser, and G. Stehr.** 1991. Classification of eight new species of ammonia-oxidizing bacteria: *Nitrosomonas communis* sp. nov., *Nitrosomonas ureae* sp. nov., *Nitrosomonas aestuarii* sp. nov., *Nitrosomonas marina* sp. nov., *Nitrosomonas nitrosa* sp. nov., *Nitrosomonas eutropha* sp. nov., *Nitrosomonas oligotropha* sp. nov., and *Nitrosomonas halophila* sp. nov. J. Gen. Microbiol. **137:**1689–1699.
24. **Larson, M. A., and B. J. Marinas.** 2003. Inactivation of *Bacillus subtilis* spores with ozone and monochloramine. Water Res. **37:**833–844.
25. **LeChevallier, M. W., C. D. Cawthon, and R. G. Lee.** 1988. Inactivation of biofilm bacteria. Appl. Environ. Microbiol. **54:**2492–2499.
26. **Lee, W., P. Westerhoff, X. Yang, and C. Shang.** 2007. Comparison of colorimetric and membrane introduction mass spectrometry techniques for chloramine analysis. Water Res. **41:**3097–3102.
27. **Lloyd, D., and A. J. Hayes.** 1995. Vigour, vitality and viability of microorganisms. FEMS Microbiol. Lett. **133:**1–7.
28. **Lunn, D. J., A. Thomas, N. Best, and D. Spiegelhalter.** 2000. WinBUGS—a Bayesian modelling framework: concepts, structure, and extensibility. Stat. Comput. **10:**325–337.
29. **Nocker, A., and A. K. Camper.** 2006. Possible errors in the interpretation of ethidium bromide and PicoGreen DNA staining results from ethidium monoazide-treated DNA. Appl. Environ. Microbiol. **72:**6861–6862.
30. **Nocker, A., C. Y. Cheung, and A. K. Camper.** 2006. Comparison of propidium monoazide with ethidium monoazide for differentiation of live vs. dead bacteria by selective removal of DNA from dead cells. J. Microbiol. Methods **67:**310–320.
31. **Nocker, A., K. Sossa, and A. K. Camper.** 2007. Molecular monitoring of disinfection efficacy using propidium monoazide in combination with quantitative PCR. J. Microbiol. Methods **70:**252–260.
32. Reference deleted.
33. **Oldenburg, P. S., J. M. Regan, G. W. Harrington, and D. R. Noguera.** 2002. Kinetics of *Nitrosomonas europaea* inactivation by chloramine. J. Am. Water Works Assoc. **94:**100–110.
34. **Prosser, J. I.** 1989. Autotrophic nitrification in bacteria. Adv. Microb. Physiol. **30:**125–181.
35. **R Development Core Team.** 2008. R: a language and environment for statistical computing. R Foundation for Statistical Computing, Vienna, Austria.
36. **Regan, J. M., A.-Y. Cho, S. Kim, and C. D. Smith.** 2007. Monitoring ammonia-oxidizing bacteria in chloraminated distribution systems. AWWA Research Foundation, Denver, CO.
37. **Regan, J. M., G. W. Harrington, H. Baribeau, R. D. Leon, and D. R. Noguera.** 2003. Diversity of nitrifying bacteria in full-scale chloraminated distribution systems. Water Res. **37:**197–205.
38. **Regan, J. M., G. W. Harrington, and D. R. Noguera.** 2002. Ammonia- and nitrite-oxidizing bacterial communities in a pilot-scale chloraminated drinking water distribution system. Appl. Environ. Microbiol. **68:**73–81.
39. **Reichert, P.** 1994. AQUASIM—a tool for simulation and data analysis of aquatic systems. Water Sci. Technol. **30:**21–30.
40. **Rennecker, J. L., B. Corona-Vasquez, A. M. Driedger, S. A. Rubin, and B. J. Marinas.** 2001. Inactivation of *Cryptosporidium parvum* oocysts with sequential application of ozone and combined chlorine. Water Sci. Technol. **43:**167–170.
41. **Rennecker, J. L., A. M. Driedger, S. A. Rubin, and B. J. Marinas.** 2000. Synergy in sequential inactivation of *Cryptosporidium parvum* with ozone/free chlorine and ozone/monochloramine. Water Res. **34:**4121–4130.
42. **Rennecker, J. L., J. H. Kim, B. Corona-Vasquez, and B. J. Marinas.** 2001. Role of disinfectant concentration and pH in the inactivation kinetics of *Cryptosporidium parvum* oocysts with ozone and monochloramine. Environ. Sci. Technol. **35:**2752–2757.
43. **Seidel, C. J., M. J. McGuire, R. S. Summers, and S. Via.** 2005. Have utilities switched to chloramines? J. Am. Water Works Assoc. **97:**87–97.
44. **Severin, B. F., M. T. Suidan, and R. S. Engelbrecht.** 1984. Series-event kinetic model for chemical disinfection. J. Environ. Eng. **110:**430–439.
45. **Sivaganesan, M., N. J. Adcock, and E. W. Rice.** 2006. Inactivation of Bacillus globigii by chlorination: a hierarchical Bayesian model. J. Water Supply Res. Technol. **55:**33–43.
46. **Sivaganesan, M., E. W. Rice, and B. J. Marinas.** 2003. A Bayesian method of estimating kinetic parameters for the inactivation of *Cryptosporidium parvum* oocysts with chlorine dioxide and ozone. Water Res. **37:**4533–4543.
47. **Siyikanchana, K., J. L. Shisler, and B. J. Marinas.** 2008. Inactivation kinetics of adenovirus serotype 2 with monochloramine. Water Res. **42:**1467–1474.
48. **Tchobanoglous, G., F. L. Burton, and H. D. Stensel.** 2003. Wastewater engineering: treatment and reuse, 4th ed. The McGraw-Hill Companies, Inc., New York, NY.
49. **USEPA.** 2005. Economic analysis for the final stage 2 disinfectants and disinfection byproducts. Rule 815-R-05-010. USEPA, Washington, DC.
50. **Venables, W. N., and B. D. Ripley.** 2002. Modern applied statistics with S, 4th ed. Springer, New York, NY.
51. **Vikesland, P. J., K. Ozekin, and R. L. Valentine.** 2001. Monochloramine decay in model and distribution system waters. Water Res. **35:**1766–1776.
52. **Wei, J. H., and S. L. Chang.** 1975. A multi-Poisson distribution model for treating disinfection data, p. 425. *In* J. D. Johnson (ed.), Disinfection: water and wastewater. Ann Arbor Science Publishers, Ann Arbor, MI.
53. **White, G. C.** 1999. Handbook of chlorination and alternative disinfectants, 4th ed. John Wiley & Sons, Inc., New York, NY.
54. **Wilczak, A., J. G. Jacangelo, J. P. Marcinko, L. H. Odell, G. J. Kirmeyer, and R. L. Wolfe.** 1996. Occurrence of nitrification in chloraminated distribution systems. J. Am. Water Works Assoc. **88:**74–85.